Northern Hemisphere temperature reconstruction during the last millennium using multiple annual proxies

Feng Shi[1,2], Bao Yang[2,*], Aurélien Mairesse[3], Lucien von Gunten[4], Jianping Li[1], Achim Bräuning[5], Fengmei Yang[6], Xia Xiao[1]

[1]State Key Laboratory of Numerical Modeling for Atmospheric Sciences and Geophysical Fluid Dynamics,
Institute of Atmospheric Physics, Chinese Academy of Sciences, 100029 Beijing, PR China

[2]Key Laboratory of Desert and Desertification, Cold and Arid Regions Environmental and Engineering Research Institute,
Chinese Academy of Sciences, 730000 Lanzhou, PR China

[3]Georges Lemaître Centre for Earth and Climate Research, Earth and Life Institute, Université catholique de Louvain,
1348 Louvain-la-Neuve, Belgium

[4]Oeschger Centre for Climate Change Research & Institute of Geography, University of Bern, 3012 Bern, Switzerland

[5]Institute of Geography, University of Erlangen-Nürnberg, 91054 Erlangen, Germany

[6]China Meteorological Administration Training Centre, 100081 Beijing, PR China,

ABSTRACT: Previous studies have either exclusively used annual tree-ring data or have combined tree-ring series with other, lower temporal resolution proxy series. Both approaches can lead to significant uncertainties, as tree-rings may underestimate the amplitude of past temperature variations, and the validity of non-annual records cannot be clearly assessed. In this study, we assembled 45 published Northern Hemisphere (NH) temperature proxy records covering the past millennium, each of which satisfied 3 essential criteria: the series must be of annual resolution, span at least a thousand years, and represent an explicit temperature signal. Suitable climate archives included ice cores, varved lake sediments, tree-rings and speleothems. We reconstructed the average annual land temperature series for the NH over the last millennium by applying 3 different reconstruction techniques: (1) principal components (PC) plus second-order autoregressive model (AR2), (2) composite plus scale (CPS) and (3) regularized errors-in-variables approach (EIV). Our reconstruction is in excellent agreement with 6 climate model simulations (including the first 5 models derived from the fifth phase of the Coupled Model Intercomparison Project (CMIP5) and an earth system model of intermediate complexity (LOVECLIM), showing similar temperatures at multidecadal timescales; however, all simulations appear to underestimate the temperature during the Medieval Warm Period (MWP). A comparison with other NH reconstructions shows that our results are consistent with earlier studies. These results indicate that well-validated annual proxy series should be used to minimize proxy-based artifacts, and that these proxy series contain sufficient information to reconstruct the low-frequency climate variability over the past millennium.

KEY WORDS: Climate change · Global warming · Palaeoclimatology · Temperature reconstruction

1. INTRODUCTION

Assessing the rapid warming in the 20th century, which is unprecedented during the last millennium, continues to be one of the highest priorities for climatologists. One approach to this is to compare the current and past natural variations of climate as reconstructed from proxy data derived from natural archives (e.g. tree-rings, ice cores, speleothems and marine or lake sediments). Numerous proxy-based

regional to global climate reconstructions have already been published (e.g. Jones et al. 1998, Mann et al. 1998, 1999, 2008, 2009, Crowley & Lowery 2000, Briffa et al. 2001, Esper et al. 2002a, Mann & Jones 2003, Cook et al. 2004a, Moberg et al. 2005, D'Arrigo et al. 2006, Osborn & Briffa 2006, Hegerl et al. 2007, Ammann & Wahl 2007, Kaufman et al. 2009, Ljungqvist 2010). However, the selection criteria for paleo-temperature proxy series can significantly affect these large-scale composite temperature reconstructions (Küttel et al. 2007, Mann 2007, Jones et al. 2009, von Storch et al. 2009).

Two different approaches have usually been used to screen the predicted proxy records: either (1) only annual tree-ring data were used, or (2) tree-ring series were combined with non-annual records (see Table 1). The advantages of tree-ring data are that their chronologies have exact dating control and annual resolution, and their temperature signals are usually well understood and can be validated using meteorological data (Hughes 2011). In addition, tree-ring records are widespread for the Northen Hemisphere (NH). The problem with tree-ring series is that the low-frequency climate signal, longer than the age of the tree, is not well preserved, or, if present, it would need to be statistically extracted from the raw data (Cook et al. 1995, Briffa & Melvin 2011). Alternative proxy data (e.g. ice cores, speleothems, varved lake or marine sediments) are good proxies for the low-frequency temperature variability, and invariably come from regions where long tree-ring records are not available. However, the problem with those records is that most are not annually resolved and their quality is hard to assess because they usually cannot be validated using annual meteorological

data. Therefore, both of these approaches have associated problems, as a pure tree-ring reconstruction may not reproduce the amplitude of past temperature changes correctly while non-annual data may introduce false or at least unvalidated information. New, non tree-ring records with annual resolution have recently been published. Thus, for this study, we assembled 45 proxy records including the tree-ring data and other proxy series with annual resolution to combine the advantages of all types of climate archives (Table 2), without their usual weaknesses.

Statistical techniques also have an important role in paleoclimate reconstruction (Christiansen 2011, McShane & Wyner 2011). Therefore, 3 different statistical techniques were used to reconstruct the annually resolved NH mean land temperature over the past 1000 yr, allowing us to analyze the effects of the different methods. Finally, we compared our reconstruction with other NH temperature reconstruction series and with 6 climate model simulations to assess its quality and reliability.

2. DATA AND METHODS

2.1. Instrumental and proxy data

Paleoclimate reconstructions may suffer from an aliasing effect when proxy data series with different temporal resolutions and different lengths are mixed (Mann et al. 2008). In this paper, criteria for the selection of the proxy records were very strict to minimize such effects. We only used proxy data series with annual resolution, which span >1000 yr, and represent an explicit temperature signal. For each research area, we considered only the newest data available and selected the data to ensure a uniform spatial distribution (Fig. 1, Table 2). Restricting data sets to those spanning >1000 yr was necessary to avoid heterogeneity in data set variance.

We started our proxy data collection using the large data set of climate records compiled by Mann et al. (2008), who collected 79 proxy records spanning >1000 yr to reconstruct NH temperatures. Of these series, 60 were not retained for this study, as they did not meet our very restrictive standards: e.g. some poor-quality data

Table 1. Number and types of data series used in multi-proxy Northern Hemisphere (NH) reconstructions (see Fig. 4). Only proxy series spanning at least 1000 yr were considered

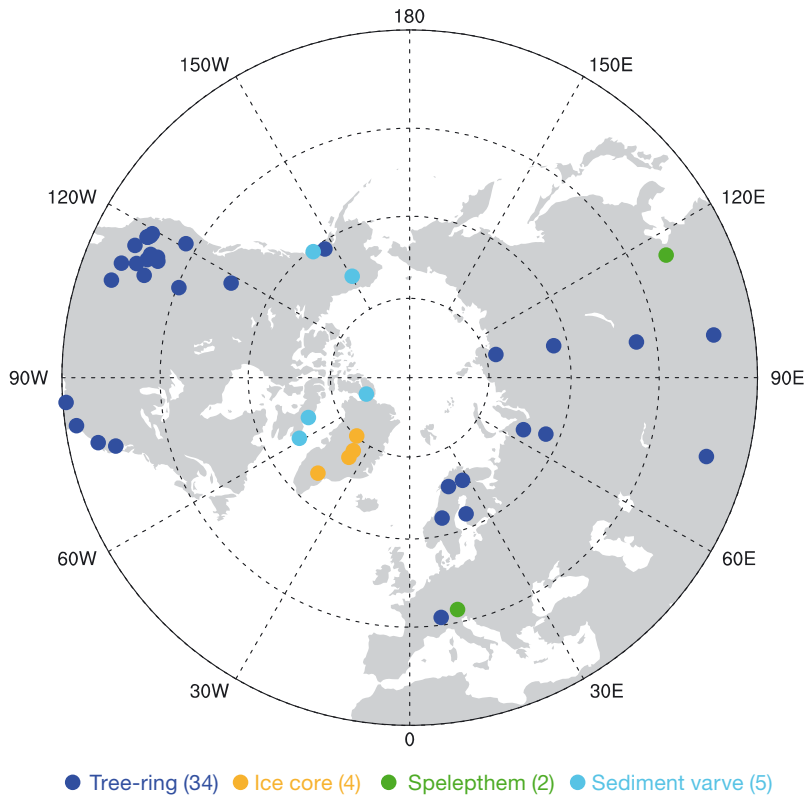| | Type of proxy | | Resolution | | Total |
	Dendro	Others	Annual	Non-annual	
This study	34	11	45	0	45
Ammann & Wahl (2007)	28	0	28	0	28
Christiansen & Ljungqvist (2012)	9	23	16	16	32
Crowley & Lowery (2000)	5	8	6	7	13
Esper et al. (2002a)	14	0	14	0	14
Hegerl et al. (2007)	11	3	0	14	14
Jones et al. (1998)	2	1	3	0	3
Ljungqvist (2010)	11	19	16	14	30
Mann et al. (1999)	28	0	28	0	28
Mann et al. (2008)	18	28	30	16	46
McShane & Wyner (2011)	62	33	77	18	95
Moberg et al. (2005)	7	11	8	10	18

Fig. 1. Geographical distribution of the 45 records used in this study. Listed in Table 2

with a coarse resolution. Regional curve standardization (RCS) is an efficient method for preserving the low-frequency signal in the raw data (Briffa & Melvin 2011). We gave priority to the collection of RCS chronologies to better preserve the low-frequency signals.

Prior to a more in-depth examination of the series, we excluded 33 tree-ring records from the Mann et al. (2008) dataset, because they did not meet the minimal replication required for tree-ring series used in this study (5 independent contributing cores). Furthermore, 16 records with a non-annual resolution were excluded. For example, we did not use the lake sediment data derived from Lake Korttajärvi, as the sedimentation has been affected by human activity since the early 18th century (Tiljander 2005). Briffa et al.'s (1992) and Grudd's (2008) Fennoscandian tree-ring sampling areas are the same (Torneträsk, Northern Sweden), but the Grudd (2008) record was updated from AD 501 to 2004 using new samples from 35 relatively young trees. This new Torneträsk tree-ring maximum latewood density (MXD) record includes samples from a total of 100 trees and covers the period AD 441–2004. Therefore, we used the most up-to-date data from Grudd (2008). For Greenland, we used Vinther et al.'s (2010) annually

resolved oxygen isotope record from ice cores. We did not use the older records published by Fisher et al. (1996) and Meese et al. (1994). The record compiled by Qian et al. (2003) represents centennial-scale dry–wet variations in East Asia, but not a specific temperature signal; it was thus not used in this study. Naurzbaev & Vaganov (2000) and Naurzbaev et al. (2002) both studied tree-rings in eastern Taimyr; the newer data by Naurzbaev et al. (2002) were used here. Also not considered for this study were the Scottish speleothem data published by Proctor et al. (2000, 2002) as the sensitivity of this archive to temperature is weak (strong negative correlation with precipitation). The latest update of the Yamal tree ring data (Briffa et al. 2008) used the RCS chronology and better reflects low frequency climate signals than former versions of the record (Briffa 2000, Hantemirov & Shiyatov 2002). The DYE-3 ice core data (Andersen et al. 2006) have been corrected for upstream depletion of $\delta^{18}O$ (Vinther et al. 2010). Consequently, only 19 of these 79 proxy series were in common with both the present and the Mann et al. (2008) reconstructions. We also collected 26 other records, resulting in a total of 45 series used for our temperature reconstruction (Table 2). All references for the 45 proxies come from 21 studies (see Table 2). Here, every series was required to exceed a 90% confidence level with either one of the 2 closest instrumental temperature grid points over the calibration interval to ensure that it had a significant statistical relationship with the local instrumental temperature signal.

Table 2 shows that the proxy records represent responses to temperature in different seasons, because of their variable local environments. For example, some tree-ring data strongly reflect the temperature of the growing season, while other tree-ring data also respond to mean annual temperature. The multidecadal variability of annual temperature and other season temperatures is usually synchronized (Jones et al. 2012). Thus, for consistency, all records were considered to approximately represent an entire year's temperature signal.

For calibration and verification purposes, we extracted the instrumental land-only NH temperature

Table 2. List of 45 annually resolved proxy records from the Northern Hemisphere (NH) used in this study. MXD: maximum latewood density; TRW: tree-ring width; RCS: regional curve standardization; Sp: speleothems; V: varved lake sediments; ITRDB: international tree-ring data bank; ND: not described; Δ: dating uncertainty

No.	Location	Latitude	Longitude	Proxy type	Season	Explained variance	Δ (yr)	Period covered	Reference
1	Torneträsk, Northern Sweden	68°21'N–68°31'N	19°45'E–19°80'E	MXD	Apr–Aug	0.4	±0	501–2004	Grudd (2008)
2	Swiss Alps	46°25'N	7°49'E	MXD	Jun–Sep	0.49	±0	755–2004	Büntgen et al. (2006)
3	Canadian Rockies	52°N	117°W	MXD	May–Aug	0.53	±0	950–1994	Luckman & Wilson (2005)
4	Tibetan Plateau, China	35°50'N–36°30'N	97°40'E–98°20'E	TRW	Annual	0.48	±0	1–1999	Liu et al. (2009)
5	Northwest Karakorum, Mongolia	35°N–37°N	74°E–76°E	TRW	Annual	0.43	±0	618–1993	Esper et al. (2002b)
6	Polar Urals, Russia	66°52'N	65°38'E	TRW	May–Sep	ND	±0	778–1990	Esper et al. (2002a)
7	Jämtland, Sweden	63°10'N	12°25'E–13°35'E	TRW–RCS	Jun–Aug	0.40	±0	1–888, 908–1999	Linderholm & Gunnarson (2005)
8	Gulf of Alaska, USA	55°–62°N	131°–153°W	MXD	Jan–Sep	ND	±0	724–2000	D'Arrigo et al. (2006)
9	Taimyr peninsula, Russia	70°30'N–73°00'N	105°E	TRW–RCS	Jun–Aug	0.45	±0	1–1996	Naurzbaev et al. (2002)
10	Fennoscandia	62°5'N	22°5'E	TRW–RCS	Jun–Aug	0.19	±0	1–1997	Briffa et al. (2008)
11	Yamal, Russia	62°5'N	67°5'E	TRW–RCS	Jun–Jul	0.31	±0	1–1996	Briffa et al. (2008)
12	Avam–Taimyr, Russia	62°5'N	102°5'E	TRW–RCS	Jul	0.15	±0	1–2000	Briffa et al. (2008)
13	Campito mountain, USA	37°5'N	118°22'W	TRW	ND	ND	±0	626–1983	ITRDB, ca533
14	Sheep mountain, USA	37°37'N	118°22'W	TRW	ND	ND	±0	1–1990	ITRDB, ca534
15	Methuselah walk, USA	37°43'N	118°17'W	TRW	ND	ND	±0	1–1979	ITRDB, ca535
16	Spillway lake, USA	37°83'N	119°22'W	TRW	ND	ND	±0	800–1996	ITRDB, ca606
17	Glass Mountain, USA	37°75'N	118°68'W	TRW	ND	ND	±0	680–1998	ITRDB, ca633
18	Choctawhatchee River, USA	30°47'N	85°88'W	TRW	ND	ND	±0	899–1992	ITRDB, fl001
19	North Fork Ridge, USA	45°3'N	111°33'W	TRW	ND	ND	±0	500–1998	ITRDB, mt111
20	Black River, USA	34°32'N	78°22'W	TRW	ND	ND	±0	365–1985	ITRDB, nc008
21	El malpais national monument, USA	34°97'N	108°1'W	TRW	ND	ND	±0	1–1992	ITRDB, nm572
22	Pearl peak, USA	40°23'N	115°53'W	TRW	ND	ND	±0	320–1985	ITRDB, nv512
23	Pearl peak, USA	40°55'N	114°82'W	TRW	ND	ND	±0	302–1985	ITRDB, nv514
24	Indian garden, USA	39°08'N	115°43'W	TRW	ND	ND	±0	1–1980	ITRDB, nv515
25	Hill 10842, Nevada, USA	38°93'N	114°23'W	TRW	ND	ND	±0	1–1984	ITRDB, nv516
26	Springs mountains lower, Nevada, USA	36°32'N	115°7'W	TRW	ND	ND	±0	320–1984	ITRDB, nv517
27	Table Rock/Arrow Gap, USA	43°18'N	120°9'W	TRW	ND	ND	±0	530–1996	ITRDB, or062
28	Wild horse ridge, USA	39°42'N	111°07'W	TRW	ND	ND	±0	286–1985	ITRDB, ut508
29	Mammoth creek, USA	37°65'N	112°67'W	TRW	ND	ND	±0	1–1989	ITRDB, ut509
30	San Francisco peaks, USA	35°5'N	111°67'W	TRW	ND	ND	±0	548–1983	ITRDB, az510
31	Altamaha river, USA	31°62'N	81°8'W	TRW	ND	ND	±0	929–1985	ITRDB, ga002

Table 2 (continued)

No.	Location	Latitude	Longitude	Proxy type	Season	Explained variance	Δ (yr)	Period covered	Reference
32	Blackwater river, USA	36°78'N	76°88'W	TRW	ND	ND	±0	932–1985	ITRDB, va021
33	Laanila, northern Finland	68°28'N–68°31'N	27°16'E–27°24'E	Height-increment record	Jun–Aug	0.36	±0	745–2000	Lindholm et al. (2011)
34	Solongotyn Davaa, Mongolia	48°3'N	98°93'E	TRW	Jul	0.33	±0	264–1998	D'Arrigo et al. (2001)
35	GRIP, Greenland	72°58'N	37°64'W	Ice core δ^{18}O	May–Oct	ND	±0	551–1979	Vinther et al. (2010)
36	DYE-3, Greenland	65°18'N	43°83'W	Ice core δ^{18}O	May–Oct	ND	±0	551–1978	Vinther et al. (2010)
37	Crete, Greenland	71°12'N	37°32'W	Ice core δ^{18}O	May–Oct	ND	±0	552–1973	Vinther et al. (2010)
38	NGRIP, Greenland	75°10'N	42°32'W	Ice core δ^{18}O	Annual	ND	±21	5–2000	Vinther et al. (2006)
39	Beijing, China	39°54'N	116°23'E	Sp	May–Aug	0.3	±5	1–1986	Tan et al. (2003)
40	Central Alps	47°05'N	11°40'E	Sp	Annual	ND	<4	1–1935	Mangini et al. (2005)
41	Canadian Arctic	81°21'N	69°32'W	V	Jul	ND	ND	1–1969, 1990–2000	Cook et al. (2009)
42	Canadian Arctic	69°52'N	68°5'W	V	Jul–Sep	0.20	ND	971–2000	Thomas & Briner (2009)
43	Southern Alaska, USA	60°47'N	142°57'W	V	May–Jun	0.05	±32	442–1998	Loso (2009)
44	Canadian Arctic	66°4'N	61°21'W	V	Jun–Aug	0.30	±80	752–1992	Moore et al. (2001)
45	Alaska, USA	68°09'N	150°47'W	V	Jun–Aug	0.10	±45	9–2000	Bird et al. (2009)

data for the period AD 1850 to 2006 from the University of East Anglia (Climatic Research Unit [CRU], Norwich, UK; www.cru.uea.ac.uk/cru/data/temperature) instrumental surface-air temperature dataset (CRUTEM3v) (Brohan et al. 2006).

2.2. Statistical methods

Three different reconstruction methodologies were used to reconstruct NH temperatures during the last 1000 yr: multivariate principal component regression (PCR), composite-plus-scaling (CPS) and the regularized errors-in-variables approach (EIV).

Principal components (PC) regression has been used in climate reconstruction research for many years (Cook et al. 1994, 2004b, Luterbacher et al. 2004, Riedwyl et al. 2009). It is well known that there is no single objective way by which to select the PCs (Wilks 2006, McShane & Wyner 2011). According to the cross-validated root mean square error (RMSE) results, the first 10 PCs of the proxy record dataset and a second-order autoregressive (AR2) model were retained (McShane & Wyner 2011). The AR2 can be used to statistically and optimally reduce the uncertainty of the regression equation errors (McShane & Wyner 2011). The model was fitted to the period AD 1850–1998 and used to reconstruct the period AD 998–1849. A Bayesian algorithm was used to estimate parameter uncertainty and residual variance using McShane & Wyner's (2011) method, yielding a much wider standard error because of noise in the proxy data and uncertainty in the relationship between the proxy data and instrumental data (McShane & Wyner 2011). The likelihood is given by McShane & Wyner (2011):

$$T_t = \beta_0 + \sum_{i=1}^{10} \beta_i (PC)_{t,i} + \beta_{11} T_{t+1} + \beta_{12} T_{t+2} + \varepsilon_t \quad (1)$$

where T_t represents the CRU NH annual land temperature in year t and $(PC)_{t,i}$ is the value of principal component i in year t. The innovations ε_t are assumed to be independent and identically distributed normal draws, $\varepsilon_t \in N(0, \sigma^2)$. All parameters are defined according to McShane & Wyner (2011), and the computational code for this method is available in their supplement.

Northern Hemisphere annual mean land temperatures were reconstructed by an AR2 model with the first 10 PCs of the dataset. The posterior was estimated using Just Another Gibbs Sampler (JAGS) (Plummer 2003) and Markov Chain Monte Carlo (MCMC) method over the calibration period (AD

1850–1998). The 95% confidence interval was calculated after 100 iterations.

PCR using simple linear regression of PCs of the proxy network and instrumental data suffers from known biases, including the underestimation of variance (von Storch et al. 2004, Hegerl et al. 2006, Neukom et al. 2011). To avoid this potential loss of variance, we also used CPS by matching the variance of the composited predictor data against the predictand in the calibration period (Jones et al. 1998, Esper et al. 2005). This is sometimes called the composite matching variance method (von Storch et al. 2009). Moreover, EIV with truncated total least squares was used to avoid overfitting in the regressions (Schneider 2001, Rutherford et al. 2005, Mann 2007, Mann et al. 2008, 2009, Riedwyl et al. 2008, 2009, Neukom et al. 2011). For a general comparison and description of the 3 approaches we refer to McShane & Wyner (2011) and corresponding discussion articles (Schmidt et al. 2011, Smerdon 2011, Tingley 2011). The procedures for all the methods are available in the supplements to original papers in the references.

2.3. Climate models

In order to assess whether our reconstructions are consistent with the model physics, a comparison is carried out with the climate of the last millennium assessed by the 6 following models: MPI-ESM-P (Jungclaus et al. 2010), CCSM4 (Gent et al. 2011), GISS-E2-R (Schmidt et al. 2006), FGOALS-g1 (Zhou et al. 2008), BCC-CSM1.1 (Wu et al. 2010) and LOVECLIM1.2 (Goosse et al. 2010). These results are the stacked reconstruction of the Paleo Modelling Intercomparison Project Phase 3 (PMIP3) (Schmidt et al. 2012) last millennium simulation and the CMIP5 historical run. The results for these two projects are available via the Earth System Grid Federation portal (http://pcmdi9.llnl.gov/esgf-web-fe/) except for LOVE-CLIM, available at http://www.climate.be/lm/.

3. RESULTS AND DISCUSSION

Northern Hemisphere annual mean land temperatures anomalies (with respect to AD 1961 to 1990) over the last 1000 yr, reconstructed with 3 statistical approaches (PC10+AR2, CPS and EIV) are shown in Fig. 2a. The model was fitted to the period AD 1850–1998 and reconstructed for AD 998–1849. A Medieval Warm Period (MWP) prior to AD 1100, a

colder Little Ice Age type event (LIA; AD ~1550–1750) and the 20th century warming are visible in the NH. The period of the LIA agrees with the reconstructions of Moberg et al. (2005) and Mann et al. (2008) that reveal cooler conditions in the NH during the intervals AD 1500–1600, 1400–1700 and 1500–1800. The most recent decades (AD 1920–1998) were clearly warmer than any period of the past 1000 yr. These posterior probabilities clearly support the assessments by Mann et al. (2008) and the Intergovernmental Panel for Climate Change (IPCC) AR4 (Jansen et al. 2007) stating that the current warming is unprecedented during the past 1000 yr. About 64 yr quasi-cycles are identified in the 3 reconstructions by wavelet analysis (not shown), which are not statistically significant. Fig. 2b compares the reconstructed results with the instrumental data since 1840. Note that the value of the EIV reconstruction is the same as the filtered instrumental data since 1850, because the EIV method is an algorithm for the imputation of missing values in incomplete datasets. Fig. 2b shows that the PC1+AR2 result is closer to the filtered instrumental data (i.e. the EIV result) than the CPS result. Fig. 2c shows results reconstructed using the no-dendro dataset, and Fig. 2d shows the dendro results. 'no dendro' means the results obtained using the proxy datasets after excluding the tree-ring records, and 'dendro' means the results reconstructed only using tree-ring data. Fig. 2c,d indicates that the reconstruction technique has an important effect on the reconstruction results, especially for the very small number of proxy data used in Fig. 2c. There are only 11 proxy records in the 'no-dendro' case. Overall, the results in this study are all very similar, with no distinct differences in the cold/warm phases of the reconstruction results at multidecadal timescales. However, the means and amplitudes of the 3 results are distinctly different due to the different regression equations (i.e. the transfer functions) of the 3 techniques. For example, Fig. 2b reveals that the composited proxy records obtained using PC10+AR2 and CPS are distinctly different after AD 1840. Thus, the backcasted results from these 2 methods would be inconsistent. The values of the instrumental data and proxy records during the calibration period should include their maximum and minimum values to render a stable regression equation (Fritts 1976). However, this is very difficult for paleoclimate reconstructions with short instrumental data series. The EIV result is distinctly higher than the others before AD 1700, especially during the MWP. Similar results were also found in other reconstructions. Mann et al. (2008) showed that the EIV
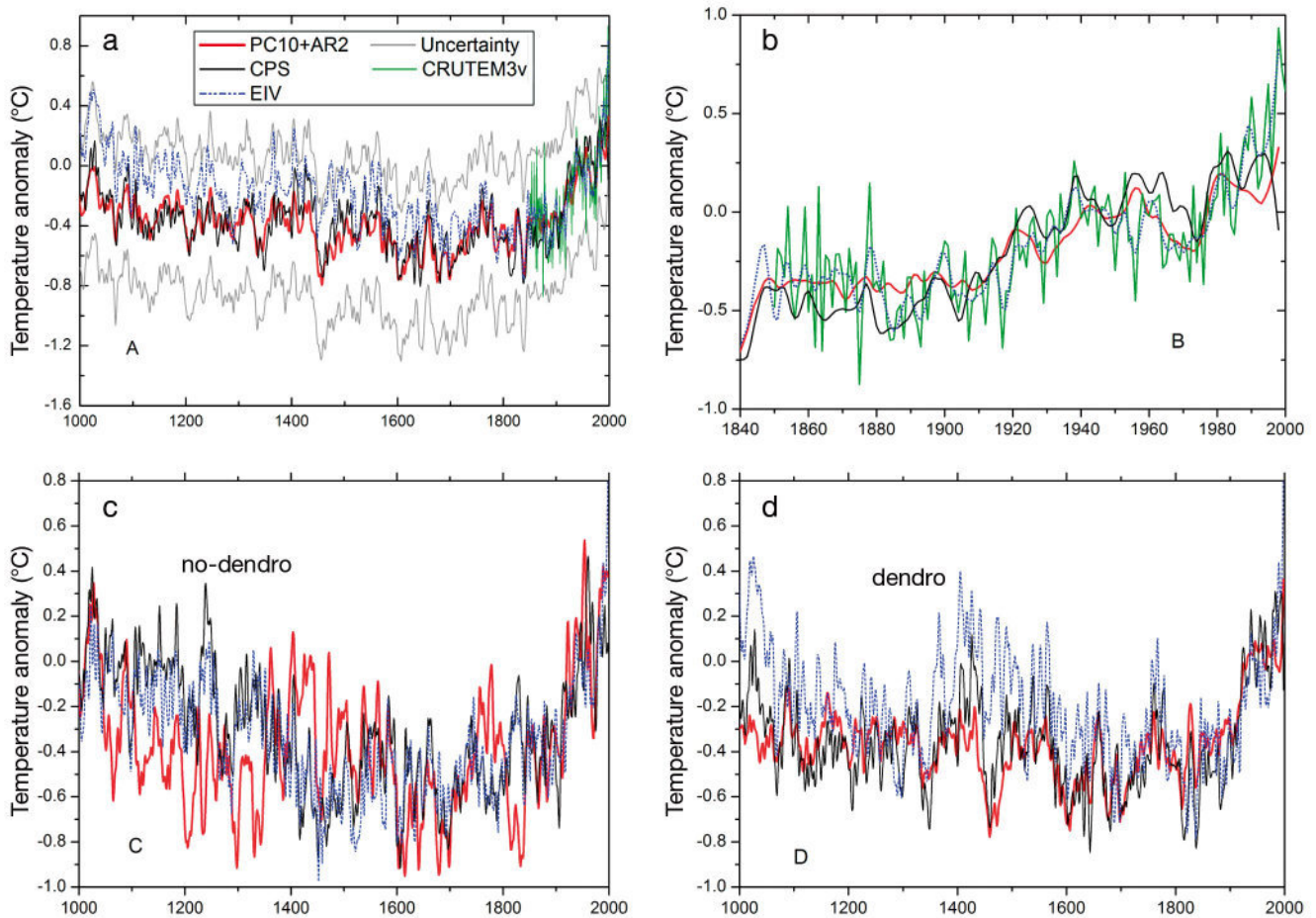
Fig. 2. Northern Hemisphere (NH) land temperature anomalies (with respect to AD 1961–1990) over the last 1000 yr reconstructed with PC10+AR2 (red solid line), CPS (black solid line) and EIV (blue dashed line). The 3 reconstruction results were smoothed by the loess method (span: 0.01). All models were fitted to the period AD 1850–1998 and reconstructed for AD 998–1849. Reconstructions for (a) AD 1000–2000 and (b) 1840–2000. Olive line: instrumental CRU NH annual mean land temperature. Gray lines: uncertainty associated with the PC10+AR2 reconstruction. Reconstructions results using (c) no-dendro data (i.e. using other types of proxy records, excluding tree-ring records), and (d) tree-ring records (dendro). Methods: 10 principal components plus second-order autoregressive model (PC10+AR2), composite plus scale (CPS) and regularized errors-in-variables approach (EIV)

method produces significantly higher temperatures in the 11th century warm period than the CPS approach. Also, Riedwyl et al. (2009) showed that PC regression underestimates the amplitude of past temperature variability, and the regularized expectation maximization (RegEM) method overestimates the temperature amplitude. This indicates that the choice of the reconstruction technique has an influence on the final paleoclimate reconstruction.

Fig. 3 compares NH land temperature anomalies (with respect to AD 1961–1990) over the last 1000 yr obtained with and without tree-ring records. 'All' means that all 45 proxy records were used to reconstruct the results. All results were smoothed by the loess method (span: 0.01), fitted for AD 1850–1998 and reconstructed for AD 998–1849. Fig. 3a shows

the PC10+AR2 results for the last 1000 yr, and Fig. 3b the same results for AD 1800–1998. Fig. 3c shows the CPS results over the last 1000 yr, and Fig. 3d the same results for AD 1800–1998. For the PC10+AR2 and CPS results, the amplitudes of the 'non-dendro' results are distinctly larger than those of the 'dendro' and 'All' results. This is consistent with the 'non-dendro' records retaining more information on the low-frequency variability. For the EIV results in Fig. 3e, all 3 results have large amplitudes; however, these results need to be further verified. It can be argued that even though the improvements and development of reconstruction techniques are very important, the most fundamental factor affecting climate reconstruction is still the quantity and quality of the input proxy data.
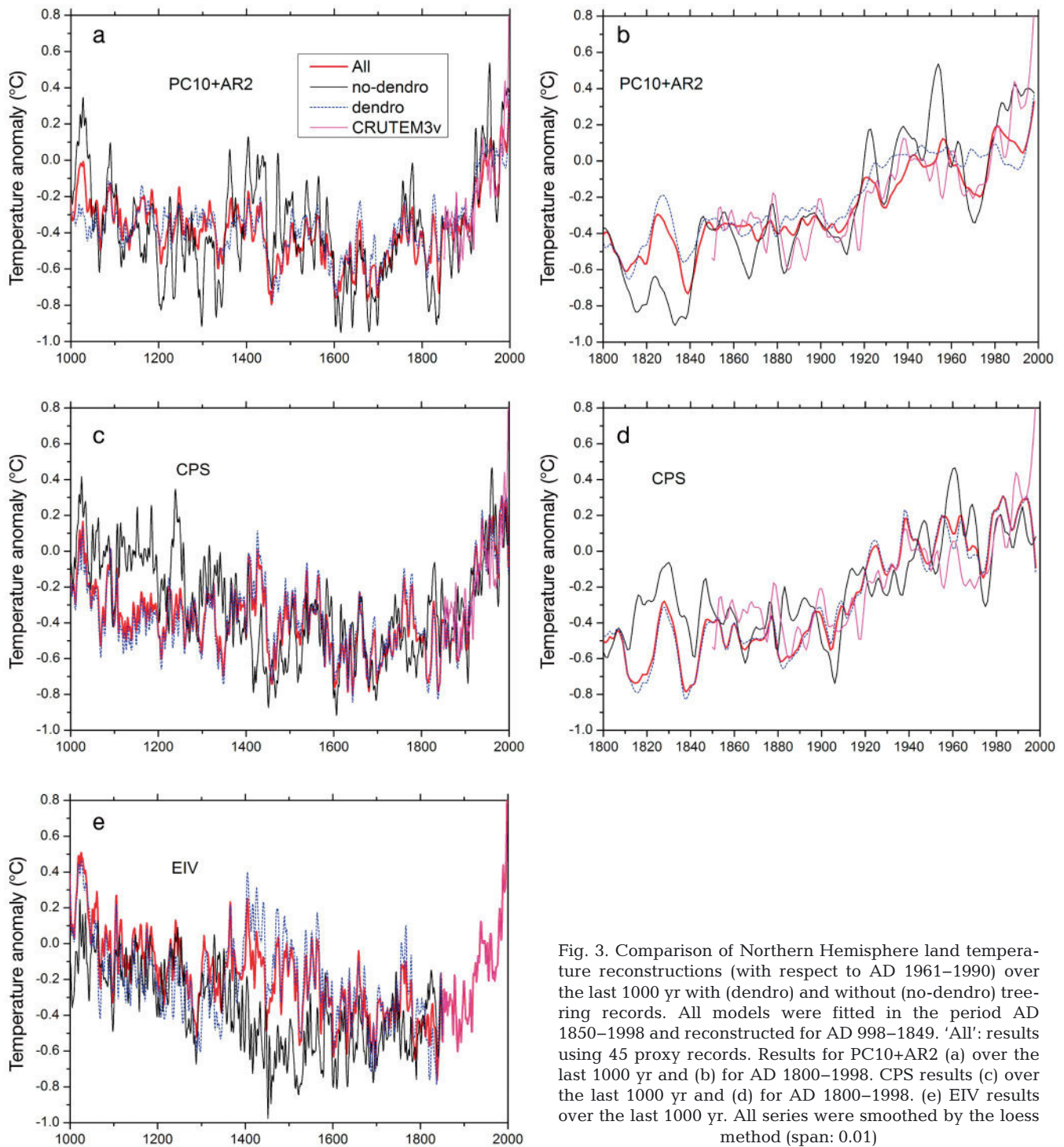
Fig. 3. Comparison of Northern Hemisphere land temperature reconstructions (with respect to AD 1961–1990) over the last 1000 yr with (dendro) and without (no-dendro) tree-ring records. All models were fitted in the period AD 1850–1998 and reconstructed for AD 998–1849. 'All': results using 45 proxy records. Results for PC10+AR2 (a) over the last 1000 yr and (b) for AD 1800–1998. CPS results (c) over the last 1000 yr and (d) for AD 1800–1998. (e) EIV results over the last 1000 yr. All series were smoothed by the loess method (span: 0.01)

Fig. 4 compares our reconstruction with other reconstructions, with 0.05 filtered values for AD 1001–1960. To facilitate comparison, every series was firstly expressed as anomalies from AD 1850–1960, and was then variance matched using the instrumental data from AD 1850–1960. Ljungqvist's (2010) result was interpolated to annual resolution and was then filtered by a 0.05 span.' Mann et al. (2008) CPS' is for the NH reconstruction result based on the CPS method, while the 'Mann et al. (2008) EIV' is for that based on the EIV method. Ammann & Wahl's (2007) curve was established by reinterpreting Mann et
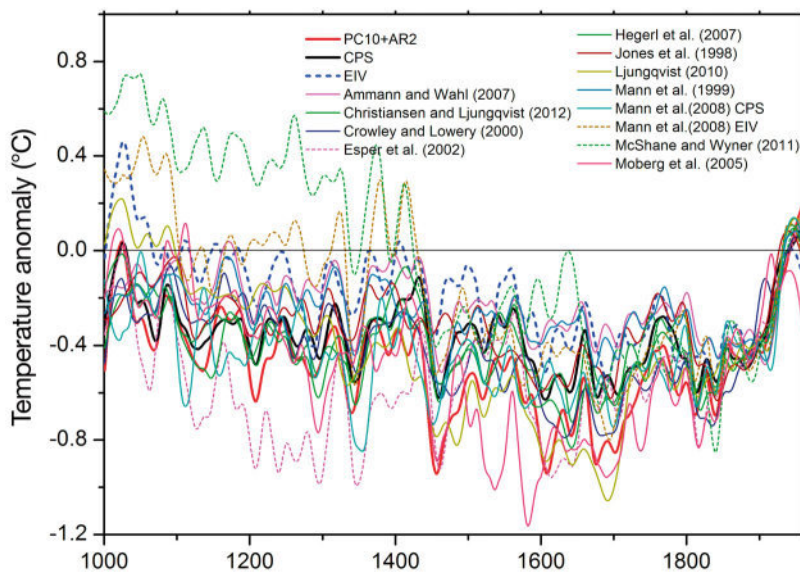
Fig. 4. Comparison of different Northern Hemisphere (NH) temperature reconstructions. All series were variance matched with the overlapping segment of CRUTEM3v instrumental NH land temperature record for 1850–1960. All reconstructions were filtered by the loess method (span: 0.05). Reconstructions: PC10+AR2 (red solid line), CPS (black solid line) and EIV (blue dashed line). Base period: AD 1001–1960

PC10+AR2 and CPS reconstructions during the MWP is generally lower than in some new reconstructions (Mann et al. 2008 EIV, Ljungqvist 2010, McShane & Wyner 2011), but the EIV result is equivalent to those of Mann et al. (2008) CPS and Ljungqvist (2010). Table 3 shows 100 yr arithmetic means of the temperature reconstructions depicted in Fig. 4. All 3 reconstructions are very similar to the reconstructions of Christiansen & Ljungqvist (2012), Crowley & Lowery (2000), Hegerl et al. (2007), Jones et al. (1998), Ljungqvist (2010) and Mann et al. (2008) CPS, which indicate lower temperatures than other reconstructions in the 11th century, when most reconstructions indicate cooler conditions than in the 20th century, except for Mann et al. (2008) EIV, Ljungqvist (2010) and McShane & Wyner (2011). The coldest century of our reconstruction was the 17th century. This result is similar to reconstructions by Christiansen & Ljungqvist (2012), Crowley & Lowery (2000), Hegerl et al. (2007), Jones et al. (1998), Mann et al. (2008) EIV and Moberg et al. (2005). Different results were found by

al. (1999), and shows little difference. These results show that our models are very similar to those from other studies in terms of the multi-decadal variability. In particular, the value of temperature variability in

Table 3. Centennial Northern Hemisphere mean temperatures. Mean base period: AD 1900–1960 in the 20th century; PC10+AR2: 10 principal components plus the second order auto-regressive model; CPS: composite plus scale; EIV: errors-in-variables approach

Century	PC10+AR2	CPS	EIV	Ammann & Wahl (2007)	Christiansen & Ljungqvist (2012)	Crowley & Lowery (2000)	Esper et al. (2002a)	Hegerl et al. (2007)	Jones et al. (1998)	Ljungqvist (2010)	Mann et al. (1999)	Mann et al. (2008) CPS	Mann et al. (2008) EIV	McShane & Wyner (2011)	Moberg et al. (2005)
11th	−0.23	−0.18	0.13	−0.12	−0.15	−0.21	−0.25	−0.22	−0.15	0.09	−0.16	−0.22	0.34	0.62	−0.10
12th	−0.36	−0.34	−0.04	−0.12	−0.33	−0.23	−0.61	−0.40	−0.26	−0.18	−0.17	−0.44	−0.05	0.42	−0.18
13th	−0.46	−0.36	−0.19	−0.18	−0.41	−0.34	−0.85	−0.43	−0.29	−0.22	−0.22	−0.35	0.01	0.36	−0.43
14th	−0.43	−0.36	−0.13	−0.16	−0.39	−0.34	−0.70	−0.41	−0.23	−0.43	−0.20	−0.52	−0.05	0.19	−0.45
15th	−0.59	−0.34	−0.13	−0.22	−0.41	−0.45	−0.61	−0.34	−0.31	−0.63	−0.36	−0.48	−0.17	−0.17	−0.52
16th	−0.56	−0.36	−0.23	−0.28	−0.42	−0.49	−0.46	−0.46	−0.42	−0.63	−0.29	−0.54	−0.41	−0.28	−0.89
17th	−0.77	−0.53	−0.39	−0.32	−0.56	−0.72	−0.76	−0.68	−0.52	−0.90	−0.35	−0.59	−0.52	−0.33	−0.85
18th	−0.58	−0.43	−0.36	−0.28	−0.46	−0.55	−0.53	−0.41	−0.31	−0.57	−0.29	−0.51	−0.45	−0.42	−0.67
19th	−0.52	−0.49	−0.41	−0.37	−0.49	−0.57	−0.54	−0.51	−0.49	−0.49	−0.39	−0.47	−0.46	−0.54	−0.56
20th	−0.12	−0.10	−0.16	−0.16	−0.12	−0.07	−0.12	−0.09	−0.07	−0.11	−0.15	−0.15	−0.12	−0.12	−0.14

Table 4. Correlation coefficient matrix between all Northern Hemisphere temperature series over the period AD 1001–1960

Correlation coefficient	PC10+AR2	CPS	EIV	Ammann & Wahl (2007)	Christiansen & Ljungqvist (2012)	Crowley & Lowery (2000)	Esper et al. (2002a)	Hegerl et al. (2007)	Jones et al. (1998)	Ljungqvist (2010)	Mann et al. (1999)	Mann et al. (2008) CPS	Mann et al. (2008) EIV	McShane & Wyner (2011)	Moberg et al. (2005)
PC10+AR2	1.00	0.90	0.72	0.70	0.88	0.85	0.64	0.79	0.74	0.85	0.75	0.65	0.71	0.59	0.77
CPS	0.90	1.00	0.76	0.74	0.91	0.79	0.72	0.87	0.74	0.72	0.74	0.65	0.70	0.52	0.67
EIV	0.72	0.76	1.00	0.65	0.77	0.70	0.38	0.62	0.65	0.73	0.59	0.48	0.79	0.79	0.70
Ammann & Wahl (2007)	0.70	0.74	0.65	1.00	0.69	0.71	0.35	0.69	0.73	0.63	0.93	0.57	0.76	0.67	0.56
Christiansen & Ljungqvist (2012)	0.88	0.91	0.77	0.69	1.00	0.81	0.71	0.87	0.74	0.82	0.71	0.72	0.73	0.58	0.73
Crowley & Lowery (2000)	0.85	0.79	0.70	0.71	0.81	1.00	0.50	0.78	0.80	0.85	0.72	0.63	0.76	0.68	0.80
Esper et al. (2002a)	0.64	0.72	0.38	0.35	0.71	0.50	1.00	0.68	0.45	0.45	0.42	0.48	0.28	0.05	0.43
Hegerl et al. (2007)	0.79	0.87	0.62	0.69	0.87	0.78	0.68	1.00	0.77	0.70	0.66	0.71	0.67	0.42	0.68
Jones et al. (1998)	0.74	0.74	0.65	0.73	0.74	0.80	0.45	0.77	1.00	0.73	0.73	0.61	0.70	0.57	0.68
Ljungqvist (2010)	0.85	0.72	0.73	0.63	0.82	0.85	0.45	0.70	0.73	1.00	0.68	0.71	0.82	0.76	0.84
Mann et al. (1999)	0.75	0.74	0.59	0.93	0.71	0.72	0.42	0.66	0.73	0.68	1.00	0.58	0.70	0.64	0.55
Mann et al. (2008) CPS	0.65	0.65	0.48	0.57	0.72	0.63	0.48	0.71	0.61	0.71	0.58	1.00	0.71	0.50	0.58
Mann et al. (2008) EIV	0.71	0.70	0.79	0.76	0.73	0.76	0.28	0.67	0.70	0.82	0.70	0.71	1.00	0.89	0.74
McShane & Wyner (2011)	0.59	0.52	0.79	0.67	0.58	0.68	0.05	0.42	0.57	0.76	0.64	0.50	0.89	1.00	0.67
Moberg et al. (2005)	0.77	0.67	0.70	0.56	0.73	0.80	0.43	0.68	0.68	0.84	0.55	0.58	0.74	0.67	1.00

Mann et al. (2008) CPS and Moberg et al. (2005), who found that the coldest episode occurred in the 16th century, and by Ammann & Wahl (2007), Mann et al. (1999) and McShane & Wyner (2011) who found the coldest interval in the 19th century. In conclusion, it appears that for the NH, the LIA maximum cooling occurred mainly during the 16th and 17th centuries. Table 4 is a correlation matrix between all the series over the common period 1001–1960. The correlation coefficients between the PC10+AR2 reconstructions and other studies are all >0.7, except for Esper et al. (2002a), Mann et al. (2008) CPS and McShane & Wyner (2011). The CPS and EIV results follow a similar pattern. These findings further illustrate that our reconstructions are well correlated with others with respect to the multi-decadal variability.

We compared our results with 6 climate model simulations over the past millennium to assess the agreement between our reconstruction and the climate physics (Fig. 5). Fig. 5 shows that the reconstructed multi-decadal variability is in very good agreement with the model results over the pre-industrial period. In addition, the amplitudes of the
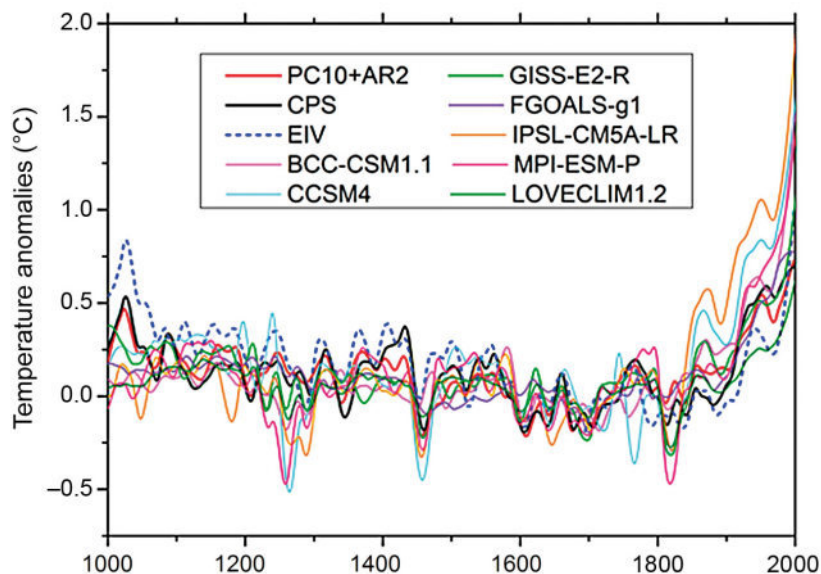

Fig. 5. Annual Northern Hemisphere temperature anomalies (with respect to AD1500–1850) smoothed with a loess filter (span: 0.05) for PC10+AR2, CPS and EIV reconstructions and 6 climate model simulations: BCC-CSM1.1, CCSM4, GISS-E2-R, FGOALS-g1, IPSL-CM5A-LR, MPI-ESM-P and LOVECLIM1.2. Base period: AD 1000–2000

models are very similar to the reconstruction except during the MWP. All curves display a general long-term cooling trend from the beginning of the millennium until AD ~1849. Some particularly cold periods are also well represented both in the simulations and in the reconstruction, such as AD ~1452–1453 and in the 17th century. However, the cooling simulated after the AD 1258 and Tambora eruptions (AD 1815) is much larger than in the reconstruction. Our results indicate that while some volcanic eruptions were captured by our reconstructions, others were less distinct. The reason is that there are some uncertainties both in the simulation and in the reconstruction (Anchukaitis et al. 2012, Mann et al. 2012). However, the paleoclimate reconstruction, to a certain extent, can capture the volcanic cooling and provides a unique opportunity to test model simulations (Braconnot et al. 2012). It is worth noting that all model simulations underestimated the temperature of the MWP. The causes of those discrepancies between the reconstruction and simulated results are difficult to assess, but we emphasize that both approaches yield the same overall pattern for the past millennium, despite their respective errors.

4. CONCLUSIONS

We selected 45 paleotemperature proxy records on the basis of 3 criteria (annual resolution, >1 millennium in length, and representing an explicit temperature signal) in order to minimize artifacts due to (1) combination of time series of different lengths or resolution and (2) non-climatic artifacts. Using these records, NH temperature over the last millennium was reconstructed using 3 different reconstruction techniques: principal component regression (PC10+AR2), composite plus scale (CPS) and the regularized errors-in-variables approach (EIV). The high quality of our reconstructions is demonstrated by the very good agreement with 6 independent climate model simulations; however, our reconstructions yielded distinctly warmer temperatures than those in all simulations during the MWP, and while our reconstructions captured the largest tropical volcanic eruption cooling event with a magnitude equivalent to that in the simulations, the other eruption cooling events were not distinct. There were notable differences between the temperature reconstructions derived from different reconstruction methods, proving that the improvement and development of reconstruction techniques is of importance for current paleoclimate reconstructions. Our results also indicate that the

amplitude of the reconstruction based only on the annually resolved dataset is equivalent to that of other reconstructions with non-annually resolved datasets. Thus, we advise the exclusive use of annually resolved proxy data which represent clearly a temperature, and which have been validated using meteorological data.

LITERATURE CITED

Ammann CM, Wahl ER (2007) The importance of the geophysical context in statistical evaluations of climate reconstruction procedures. Clim Change 85:71–88

Anchukaitis KJ, Breitenmoser P, Briffa KR, Buchwal A, and others (2012) Tree rings and volcanic cooling. Nat Geosci 5:836-837

Andersen KK, Ditlevsen PD, Rasmussen SO, Clausen HB, Vinther BM, Johnsen SJ, Steffensen JP (2006) Retrieving a common accumulation record from Greenland ice cores for the past 1800 years. J Geophys Res 111:D15106, doi:10.1029/2005JD006765

Bird BW, Abbott MB, Finney BP, Kutchko B (2009) A 2000 year varve-based climate record from the central Brooks Range, Alaska. J Paleolimnol 41:25–41

Braconnot P, Harrison SP, Kageyama M, Bartlein PJ and others (2012) Evaluation of climate models using palaeoclimatic data. Nat Clim Change 2:417–424

Briffa KR (2000) Annual climate variability in the Holocene: interpreting the message of ancient trees. Quat Sci Rev 19:87–105

Briffa KR, Melvin TM (2011) A closer look at regional curve standardization of tree-ring records: justification of the need, a warning of some pitfalls, and suggested improvements in its application. In: Hughes MK, Swetnam TW, Diaz HF (eds) Dendroclimatology: progress and prospects, Vol 11. Springer-Verlag, Berlin, p 133–145

Briffa KR, Jones PD, Bartholin TS, Eckstein D and others (1992) Fennoscandian summers from AD 500: temperature changes on short and long timescales. Clim Dyn 7: 111–119

Briffa KR, Osborn TJ, Schweingruber FH, Harris IC, Jones PD, Shiyatov SG, Vaganov EA (2001) Low-frequency

temperature variations from a northern tree ring density network. J Geophys Res D Atmospheres 106:2929–2941

Briffa KR, Shishov VV, Melvin TM, Vaganov EA and others (2008) Trends in recent temperature and radial tree growth spanning 2000 years across northwest Eurasia. Philos Trans R Soc Lond B 363:2269–2282

Brohan P, Kennedy J, Harris I, Tett S, Jones P (2006) Uncertainty estimates in regional and global observed temperature changes: a new dataset from 1850. J Geophys Res 111:D12106, doi:10.1029/2005JD006548

Büntgen U, Frank DC, Nievergelt D, Esper J (2006) Summer temperature variations in the European Alps, AD 755–2004. J Clim 19:5606–5623

Christiansen B (2011) Reconstructing the NH mean temperature: can underestimation of trends and variability be avoided? J Clim 24:674–692

Christiansen B, Ljungqvist FC (2012) The extra-tropical Northern Hemisphere temperature in the last two millennia: reconstructions of low-frequency variability. Clim Past 8:765–786

Cook ER, Briffa KR, Jones PD (1994) Spatial regression methods in dendroclimatology: a review and comparison of two techniques. Int J Climatol 14:379–402

Cook ER, Briffa KR, Meko DM, Graybill DA, Funkhouser G (1995) The 'segment length curse' in long tree-ring chronology development for palaeoclimatic studies. Holocene 5:229–237

Cook E, Esper J, D'Arrigo R (2004a) Extra-tropical Northern Hemisphere land temperature variability over the past 1000 years. Quat Sci Rev 23:2063–2074

Cook E, Woodhouse C, Eakin C, Meko D, Stahle D (2004b) Long-term aridity changes in the western United States. Science 306:1015–1018

Cook T, Bradley R, Stoner J, Francus P (2009) Five thousand years of sediment transfer in a high arctic watershed recorded in annually laminated sediments from Lower Murray Lake, Ellesmere Island, Nunavut, Canada. J Paleolimnol 41:77–94

Crowley TJ, Lowery TS (2000) How warm was the medieval warm period? Ambio 29:51–54

D'Arrigo R, Jacoby G, Frank D, Pederson N and others (2001) 1738 years of Mongolian temperature variability inferred from a tree-ring width chronology of Siberian pine. Geophys Res Lett 28:543–546

D'Arrigo R, Wilson R, Jacoby G (2006) On the long-term context for late twentieth century warming. J Geophys Res 111:D03103, doi:10.1029/2005JD006352

Esper J, Cook E, Schweingruber F (2002a) Low-frequency signals in long tree-ring chronologies for reconstructing past temperature variability. Science 295:2250–2253

Esper J, Schweingruber F, Winiger M (2002b) 1300 years of climatic history for Western Central Asia inferred from tree-rings. Holocene 12:267–277

Esper J, Frank D, Wilson R, Briffa K (2005) Effect of scaling and regression on reconstructed temperature amplitude for the past millennium. Geophys Res Lett 32:L07711, doi:10.1029/2004GL021236

Fisher DA, Koerner RM, Kuiviner K, Clausen HB and others (1996) Inter-comparison of ice core and precipitation records from sites in Canada and Greenland over the last 3500 years and over the last few centuries in detail using EOF techniques. NATO ASI Ser 1, Vol 41, Springer-Verlag, Berlin, p 297–328

Fritts H (1976) Tree rings and climate. Academic Press, London

Gent PR, Danabasoglu G, Donner LJ, Holland MM and others (2011) The community climate system model version 4. J Clim 24:4973–4991

Goosse H, Brovkin V, Fichefet T, Haarsma R and others (2010) Description of the Earth system model of intermediate complexity LOVECLIM version 1.2. Geosci Model Dev 3:603–633

Grudd H (2008) Torneträsk tree-ring width and density AD 500-2004: a test of climatic sensitivity and a new 1500-year reconstruction of north Fennoscandian summers. Clim Dyn 31:843–857

Hantemirov R, Shiyatov S (2002) A continuous multimillennial ring-width chronology in Yamal, northwestern Siberia. Holocene 12:717–726

Hegerl GC, Crowley TJ, Hyde WT, Frame DJ (2006) Climate sensitivity constrained by temperature reconstructions over the past seven centuries. Nature 440:1029–1032

Hegerl GC, Crowley TJ, Allen M, Hyde WT, Pollack HN, Smerdon J, Zorita E (2007) Detection of human influence on a new, validated 1500-year temperature reconstruction. J Clim 20:650–666

Hughes MK (2011) Dendroclimatology in high-resolution paleoclimatology. In: Hughes MK, Swetnam TW, Diaz HF (eds) Dendroclimatology: progress and prospects, Vol 11. Springer-Verlag, Berlin, p 17–36

Jansen E, Overpeck J, Briffa K, Duplessy J and others (2007) Palaeoclimate. Climate Change 2007: The Physical Science Basis. Contribution of Working Group I to the Fourth Assessment Report of the Intergovernmental Panel on Climate Change. Cambridge University Press, Cambridge

Jones PD, Briffa KR, Barnett TP, Tett SFB (1998) High-resolution palaeoclimatic records for the last millennium: interpretation, integration and comparison with General Circulation Model control-run temperatures. Holocene 8:455–471

Jones PD, Briffa KR, Osborn TJ, Lough JM and others (2009) High-resolution palaeoclimatology of the last millennium: a review of current status and future prospects. Holocene 19:3–49

Jones PD, Lister DH, Osborn TJ, Harpham C, Salmon M, Morice CP (2012) Hemispheric and large-scale land-surface air temperature variations: an extensive revision and an update to 2010. J Geophys Res 117:D05127, doi: 10.1029/2011JD017139

Jungclaus JH, Lorenz SJ, Timmreck C, Reick CH and others (2010) Climate and carbon-cycle variability over the last millennium. Clim Past 6:723–737

Kaufman DS, Schneider DP, McKay NP, Ammann CM, and others (2009) Recent warming reverses long-term Arctic cooling. Science 325:1236–1239

Küttel M, Luterbacher J, Zorita E, Xoplaki E, Riedwyl N, Wanner H (2007) Testing a European winter surface temperature reconstruction in a surrogate climate. Geophys Res Lett 34:L07710, doi:10.1029/2006GL027907

Linderholm HW, Gunnarson BE (2005) Summer temperature variability in central Scandinavia during the last 3600 years. Geogr Ann, Ser A 87:231–241

Lindholm M, Jalkanen R, Salminen H, Aalto T, Ogurtsov M (2011) The height-increment record of summer temperature extended over the last millennium in Fennoscandia. Holocene 21:319–326

Liu Y, An Z, Linderholm H, Chen D and others (2009)

Annual temperatures during the last 2485 years in the mid-eastern Tibetan Plateau inferred from tree rings. Sci China D Earth Sci 52:348–359

Ljungqvist FC (2010) A new reconstruction of temperature variability in the extra-tropical Northern Hemisphere during the last two 2 millennia. Geogr Ann, Ser A 92: 339–351

Loso M (2009) Summer temperatures during the Medieval Warm Period and Little Ice Age inferred from varved proglacial lake sediments in southern Alaska. J Paleolimnol 41:117–128

Luckman B, Wilson R (2005) Summer temperatures in the Canadian Rockies during the last millennium: a revised record. Clim Dyn 24:131–144

Luterbacher J, Dietrich D, Xoplaki E, Grosjean M, Wanner H (2004) European seasonal and annual temperature variability, trends, and extremes since 1500. Science 303: 1499–1503

Mangini A, Spötl C, Verdes P (2005) Reconstruction of temperature in the Central Alps during the past 2000 yr from a δ^{18}O stalagmite record. Earth Planet Sci Lett 235: 741–751

Mann ME (2007) Climate over the past two millennia. Annu Rev Earth Planet Sci 35:111–136

Mann ME, Jones PD (2003) Global surface temperatures over the past two millennia. Geophys Res Lett 30:1820, doi:10.1029/2003GL017814

Mann ME, Bradley RS, Hughes MK (1998) Global-scale temperature patterns and climate forcing over the past six centuries. Nature 392:779–787

Mann ME, Bradley RS, Hughes MK (1999) Northern hemisphere temperatures during the past millennium: inferences, uncertainties, and limitations. Geophys Res Lett 26:759–762

Mann ME, Zhang ZH, Hughes MK, Bradley RS, Miller SK, Rutherford S, Ni FB (2008) Proxy-based reconstructions of hemispheric and global surface temperature variations over the past two millennia. Proc Natl Acad Sci USA 105:13252–13257

Mann ME, Zhang ZH, Rutherford S, Bradley RS and others (2009) global signatures and dynamical origins of the Little Ice Age and Medieval Climate Anomaly. Science 326: 1256–1260

Mann ME, Fuentes JD, Rutherford S (2012) Underestimation of volcanic cooling in tree-ring-based reconstructions of hemispheric temperatures. Nat Geosci 5:202–205

McShane BB, Wyner AJ (2011) A statistical analysis of multiple temperature proxies: are reconstructions of surface temperatures over the last 1000 years reliable? Ann Appl Stat 5:5–44

Meese D, Gow A, Grootes P, Stuiver M and others (1994) The accumulation record from the GISP2 core as an indicator of climate change throughout the Holocene. Science 266:1680–1682

Moberg A, Sonechkin DM, Holmgren K, Datsenko NM, Karlén W (2005) Highly variable Northern Hemisphere temperatures reconstructed from low- and high-resolution proxy data. Nature 433:613–617

Moore J, Hughen K, Miller G, Overpeck J (2001) Little Ice Age recorded in summer temperature reconstruction from vared sediments of Donard Lake, Baffin Island, Canada. J Paleolimnol 25:503–517

Naurzbaev M, Vaganov E (2000) Variation of early summer and annual temperature in east Taymir and Putoran

(Siberia) over the last two millennia inferred from tree rings. J Geophys Res 105:7317–7326

Naurzbaev M, Vaganov E, Sidorova O, Schweingruber F (2002) Summer temperatures in eastern Taimyr inferred from a 2427-year late-Holocene tree-ring chronology and earlier floating series. Holocene 12:727–736

Neukom R, Luterbacher J, Villalba R, Kuttel M and others (2011) Multiproxy summer and winter surface air temperature field reconstructions for southern South America covering the past centuries. Clim Dyn 37:35–51

Osborn TJ, Briffa KR (2006) The spatial extent of 20th-century warmth in the context of the past 1200 years. Science 311:841–844

Plummer M (2003) JAGS: a program for analysis of Bayesian graphical models using Gibbs sampling. In: Hornik K, Leisch F, Zeileis A (ed) Proc 3rd Int Workshop DSC, March 20–22, Vienna

Proctor, Baker A, Barnes W (2002) A three thousand year record of North Atlantic climate. Clim Dyn 19:449–454

Proctor C, Baker A, Barnes W, Gilmour M (2000) A thousand year speleothem proxy record of North Atlantic climate from Scotland. Clim Dyn 16:815–820

Qian W, Hu Q, Zhu Y, Lee D (2003) Centennial-scale dry-wet variations in East Asia. Clim Dyn 21:77–89

Riedwyl N, Luterbacher J, Wanner H (2008) An ensemble of European summer and winter temperature reconstructions back to 1500. Geophys Res Lett 35:L20707, doi: 10.1029/2008GL035395

Riedwyl N, Kuttel M, Luterbacher J, Wanner H (2009) Comparison of climate field reconstruction techniques: application to Europe. Clim Dyn 32:381–395

Rutherford S, Mann ME, Osborn TJ, Bradley RS, Briffa KR, Hughes MK, Jones PD (2005) Proxy-based Northern Hemisphere surface temperature reconstructions: sensitivity to method, predictor network, target season, and target domain. J Clim 18:2308–2329

Schmidt GA, Ruedy R, Hansen JE, Aleinov I and others (2006) Present-day atmospheric simulations using GISS ModelE: comparison to *in situ*, satellite, and reanalysis data. J Clim 19:153–192

Schmidt GA, Mann ME, Rutherford SD (2011) Discussion of: a statistical analysis of multiple temperature proxies: are reconstructions of surface temperatures over the last 1000 years reliable? Ann Appl Stat 5:65–70

Schmidt GA, Jungclaus JH, Ammann CM, Bard E and others (2012) Climate forcing reconstructions for use in PMIP simulations of the Last Millennium (v1.1). Geosci Model Dev 5:185–191

Schneider T (2001) Analysis of incomplete climate data: estimation of mean values and covariance matrices and imputation of missing values. J Clim 14:853–871

Smerdon JE (2011) Discussion of: a statistical analysis of multiple temperature proxies: are reconstructions of surface temperatures over the last 1000 years reliable. Ann Appl Stat 5:76–79

Tan M, Liu T, Hou J, Qin X, Zhang H, Li T (2003) Cyclic rapid warming on centennial-scale revealed by a 2650-year stalagmite record of warm season temperature. Geophys Res Lett 30:1617–1620

Thomas E, Briner J (2009) Climate of the past millennium inferred from varved proglacial lake sediments on northeast Baffin Island, Arctic Canada. J Paleolimnol 41: 209–224

Tiljander M (2005) Holocene sedimentary history of annual

laminations of Lake Korttajarvi, central Finland. PhD thesis, University of Helsinki

Tingley MP (2011) Spurious predictions with random time series: the Lasso in the context of paleoclimatic reconstructions. Discussion of: A statistical analysis of multiple temperature proxies: Are reconstructions of surface temperatures over the last 1000 years reliable? Ann Appl Stat 5:83-87

Vinther BM, Clausen HB, Johnsen SJ, Rasmussen SO and others (2006) A synchronized dating of three Greenland ice cores throughout the Holocene. J Geophys Res 111: D13102, doi:10.1029/2005JD006921

Vinther BM, Jones PD, Briffa KR, Clausen HB, Andersen KK, Dahl-Jensen D, Johnsen SJ (2010) Climatic signals in multiple highly resolved stable isotope records from Greenland. Quat Sci Rev 29:522–538

von Storch H, Zorita E, Jones J, Dimitriev Y, Gonzalez-Rouco F, Tett S (2004) Reconstructing past climate from noisy data. Science 306:679–682

von Storch H, Zorita E, Gonzalez-Rouco F (2009) Assessment of three temperature reconstruction methods in the virtual reality of a climate simulation. Int J Earth Sci 98:67–82

Wahl ER, Ammann CM (2007) Robustness of the Mann, Bradley, Hughes reconstruction of Northern Hemisphere surface temperatures: examination of criticisms based on the nature and processing of proxy climate evidence. Clim Change 85:33–69

Wilks D (2006) Statistical methods in the atmospheric sciences, Vol 91. Elsevier, Amsterdam

Wu T, Yu R, Zhang F, Wang Z and others (2010) The Beijing Climate Center atmospheric general circulation model: description and its performance for the present-day climate. Clim Dyn 34:123–147

Zhou T, Wu B, Wen X, Li L, Wang B (2008) A fast version of LASG/IAP climate system model and its 1000-year control integration. Adv Atmos Sci 25:655–672